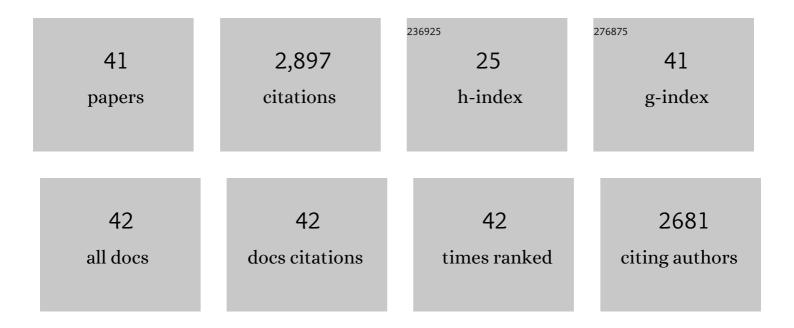
Paul R Craddock

List of Publications by Year in descending order

Source: https://exaly.com/author-pdf/9432300/publications.pdf Version: 2024-02-01



PALLE P C PADDOCK

#	Article	IF	CITATIONS
1	Robust determination of kerogen properties in organic-rich mudrocks via Raman Spectroscopy. Organic Geochemistry, 2022, 169, 104381.	1.8	4
2	Critical Practices for the Preparation and Analysis of Kerogen. Energy & Fuels, 2022, 36, 8828-8843.	5.1	5
3	Universal Curves Describing the Chemical and Physical Evolution of Type II Kerogen during Thermal Maturation. Energy & Fuels, 2020, 34, 15217-15233.	5.1	23
4	Structure-Solubility Relationships in Coal, Petroleum, and Immature Source-Rock-Derived Asphaltenes. Energy & Fuels, 2020, 34, 10825-10836.	5.1	14
5	Acid demineralization with pyrite removal and critical point drying for kerogen microstructural analysis. Fuel, 2019, 253, 266-272.	6.4	11
6	Geochemistry of hot-springs at the SuSu Knolls hydrothermal field, Eastern Manus Basin: Advanced argillic alteration and vent fluid acidity. Geochimica Et Cosmochimica Acta, 2019, 255, 25-48.	3.9	27
7	Characterization and range of kerogen properties in the Vaca Muerta Formation, Neuquén Basin, Argentina. Organic Geochemistry, 2019, 129, 42-44.	1.8	14
8	Thermal Maturity-Adjusted Log Interpretation (TMALI) in Organic Shales. Petrophysics, 2019, 60, 540-559.	0.3	4
9	Evolution of sulfur speciation in bitumen through hydrous pyrolysis induced thermal maturation of Jordanian Ghareb Formation oil shale. Fuel, 2018, 219, 214-222.	6.4	17
10	Chemical, Molecular, and Microstructural Evolution of Kerogen during Thermal Maturation: Case Study from the Woodford Shale of Oklahoma. Energy & Fuels, 2018, 32, 4859-4872.	5.1	66
11	Matrix-Adjusted Shale Porosity Measured in Horizontal Wells. Petrophysics, 2018, 3, 288-307.	0.3	4
12	Integrating Measured Kerogen Properties With Log Analysis for Petrophysics and Geomechanics in Unconventional Resources. Petrophysics, 2018, 59, 565-586.	0.3	3
13	Fast and accurate shale maturity determination by Raman spectroscopy measurement with minimal sample preparation. International Journal of Coal Geology, 2017, 173, 150-157.	5.0	107
14	Downhole Estimate of the Enthalpy Required To Heat Oil Shale and Heavy Oil Formations. Energy & Fuels, 2017, 31, 362-373.	5.1	6
15	Assessing thermal maturity beyond the reaches of vitrinite reflectance and Rock-Eval pyrolysis: A case study from the Silurian Qusaiba formation. International Journal of Coal Geology, 2017, 180, 29-45.	5.0	70
16	Comparison of Quantitative Mineral Analysis By X-Ray Diffraction and Fourier Transform Infrared Spectroscopy. Journal of Sedimentary Research, 2017, 87, 630-652.	1.6	10
17	Kerogen thermal maturity and content of organic-rich mudrocks determined using stochastic linear regression models applied to diffuse reflectance IR Fourier transform spectroscopy (DRIFTS). Organic Geochemistry, 2017, 110, 122-133.	1.8	40
18	Unusual δ 56 Fe values in Samoan rejuvenated lavas generated in the mantle. Earth and Planetary Science Letters, 2016, 450, 221-232.	4.4	64

PAUL R CRADDOCK

#	Article	IF	CITATIONS
19	Sulfur Species in Source Rock Bitumen before and after Hydrous Pyrolysis Determined by X-ray Absorption Near-Edge Structure. Energy & Fuels, 2016, 30, 6264-6270.	5.1	36
20	Impact of Laboratory-Induced Thermal Maturity on Asphaltene Molecular Structure. Energy & Fuels, 2016, 30, 7025-7036.	5.1	25
21	XANES measurements of sulfur chemistry during asphalt oxidation. Fuel, 2015, 162, 179-185.	6.4	29
22	Submarine venting of magmatic volatiles in the Eastern Manus Basin, Papua New Guinea. Geochimica Et Cosmochimica Acta, 2015, 163, 178-199.	3.9	59
23	Evolution of Kerogen and Bitumen during Thermal Maturation via Semi-Open Pyrolysis Investigated by Infrared Spectroscopy. Energy & Fuels, 2015, 29, 2197-2210.	5.1	124
24	Fe isotope fractionation during phase separation in the NaCl–H2O system: An experimental study with implications for seafloor hydrothermal vents. Earth and Planetary Science Letters, 2014, 406, 223-232.	4.4	20
25	Sulfur speciation in kerogen and bitumen from gas and oil shales. Organic Geochemistry, 2014, 68, 5-12.	1.8	62
26	The neutron scattering length density of kerogen and coal as determined by CH3OH/CD3OH exchange. Fuel, 2014, 117, 801-808.	6.4	43
27	Sulfur Chemistry of Asphaltenes from a Highly Compositionally Graded Oil Column. Energy & Fuels, 2013, 27, 4604-4608.	5.1	67
28	Abyssal peridotites reveal the near-chondritic Fe isotopic composition of the Earth. Earth and Planetary Science Letters, 2013, 365, 63-76.	4.4	149
29	Iron isotope fractionation in planetary crusts. Geochimica Et Cosmochimica Acta, 2012, 89, 31-45.	3.9	60
30	lron, zinc, magnesium and uranium isotopic fractionation during continental crust differentiation: The tale from migmatites, granitoids, and pegmatites. Geochimica Et Cosmochimica Acta, 2012, 97, 247-265.	3.9	203
31	Geochemistry of hydrothermal fluids from the PACMANUS, Northeast Pual and Vienna Woods hydrothermal fields, Manus Basin, Papua New Guinea. Geochimica Et Cosmochimica Acta, 2011, 75, 1088-1123.	3.9	185
32	Iron and carbon isotope evidence for microbial iron respiration throughout the Archean. Earth and Planetary Science Letters, 2011, 303, 121-132.	4.4	159
33	Iron Isotopic Compositions of Geological Reference Materials and Chondrites. Geostandards and Geoanalytical Research, 2011, 35, 101-123.	3.1	284
34	Rare earth element abundances in hydrothermal fluids from the Manus Basin, Papua New Guinea: Indicators of sub-seafloor hydrothermal processes in back-arc basins. Geochimica Et Cosmochimica Acta, 2010, 74, 5494-5513.	3.9	137
35	Insights to magmatic–hydrothermal processes in the Manus back-arc basin as recorded by anhydrite. Geochimica Et Cosmochimica Acta, 2010, 74, 5514-5536.	3.9	44
36	Oxygen and iron isotope constraints on near-surface fractionation effects and the composition of lunar mare basalt source regions. Geochimica Et Cosmochimica Acta, 2010, 74, 6249-6262.	3.9	62

PAUL R CRADDOCK

#	Article	IF	CITATIONS
37	Iron isotopes may reveal the redox conditions of mantle melting from Archean to Present. Earth and Planetary Science Letters, 2009, 288, 255-267.	4.4	260
38	Zinc stable isotopes in seafloor hydrothermal vent fluids and chimneys. Earth and Planetary Science Letters, 2008, 269, 17-28.	4.4	143
39	Sulfur isotope measurement of sulfate and sulfide by high-resolution MC-ICP-MS. Chemical Geology, 2008, 253, 102-113.	3.3	143
40	Permeability-porosity relationships in seafloor vent deposits: Dependence on pore evolution processes. Journal of Geophysical Research, 2007, 112, .	3.3	26
41	Controls of fluid chemistry and complexation on rare-earth element contents of anhydrite from the Pacmanus subseafloor hydrothermal system, Manus Basin, Papua New Guinea. Mineralium Deposita, 2003, 38, 916-935.	4.1	77